Synthesis, Structure, and Photoluminescent Behavior of Molecular Lanthanide-2-Thiophenecarboxylate -2,2':6',2''-Terpyridine Materials

Rami J. Batrice,[†] J. August Ridenour,[‡] R. Lee Ayscue, III,[†] Jeffery A. Bertke,[†] Karah E. Knope[†,]*

[†]Department of Chemistry, Georgetown University, 37th and O Sts., NW, Washington, D.C. 20057, USA

[‡]Department of Chemistry, The George Washington University, 800 22nd St. NW, Washington, D.C. 20052, USA

Supporting Information

Synthetic Details

[La_2(terpy)$_2$(TC)$_6$(H_2O)$_2$]•0.79H_2O (***La-1***). The dimer was synthesized according to the general procedure using 93.4 mg $LaCl_3$•7H_2O (252 μmol), 61.5 mg terpy (264 μmol), and 99.0 mg 2-HTC (773 μmol). Small, colorless rhombus-shaped crystals were collected by filtration, washed with water, dried, and collected in a 72% yield (144 mg). Elemental Analysis: Calcd. for $C_{60}H_{45.58}N_6O_{14.79}S_6La_2$: C, 46.27; H, 2.95; N, 5.40. Found: C, 46.13; H, 2.90; N, 5.38.

[(Ce_2(terpy)$_2$(TC)$_6$(H_2O)$_2$]•0.69H_2O (***Ce-1***). The dimer was synthesized according to the general procedure using 96.2 mg $CeCl_3$•7H_2O (258 μmol), 58.8 mg terpy (252 μmol), and 98.6 mg 2-HTC (769 μmol). Large yellow rhombus-shaped crystals were collected by filtration, washed with water, dried, and collected in an 85% yield (167 mg). Elemental Analysis: Calcd. for $C_{60}H_{45.38}N_6O_{14.69}S_6Ce_2$: C, 46.25; H, 2.94; N, 5.39. Found: C, 46.19; H, 2.70; N, 5.34.

[Pr_2(terpy)$_2$(TC)$_6$(H_2O)$_2$]•0.64H_2O (***Pr-1***). The dimer was synthesized according to the general procedure using 92.3 mg $PrCl_3$•7H_2O (247 μmol), 57.5 mg terpy (246 μmol), and 98.5 mg 2-HTC (769 μmol). Large pale green rhombus-shaped crystals were collected by filtration, washed with water, dried, and collected in a 79% yield (152 mg). Elemental Analysis: Calcd. for $C_{60}H_{45.28}N_6O_{14.64}S_6Pr_2$: C, 46.23; H, 2.93; N, 5.39. Found: C, 46.23; H, 2.82; N, 5.34.

[Nd_2(terpy)$_2$(TC)$_6$(H_2O)$_2$]•0.63H_2O (***Nd-1***). The dimer was synthesized according to the general procedure using 46.1 mg Nd_2O_3 (137 μmol), 61.3 mg terpy (263 μmol), and 97.4 mg 2-HTC (760 μmol). Large colorless rhombus-shaped crystals were collected by filtration, washed with water, dried, and collected in a 90% yield (178 μmol). Elemental Analysis: Calcd. for $C_{60}H_{45.26}N_6O_{14.63}S_6Nd_2$: C, 46.04; H, 2.91; N, 5.37. Found: C, 46.05; H, 2.85; N, 5.19.

[Sm_2(terpy)$_2$(TC)$_6$(H_2O)$_2$•0.42H_2O (***Sm-1***). The dimer was synthesized according to the general procedure using 100.7 mg $SmCl_3$•6H_2O (276 μmol), 59.3 mg terpy (254 μmol), and 99.4 mg 2-HTC (776 μmol). Large colorless rhombus-shaped crystals were collected by filtration, washed with water, dried, and collected in a 75% yield (153 μmol). Elemental Analysis: Calcd. for $C_{60}H_{44.84}N_6O_{14.42}S_6Sm_2$: C, 45.76; H, 2.88; N, 5.34. Found: C, 45.73; H, 2.75; N, 5.28.

[Eu_2(terpy)$_2$(TC)$_6$(H_2O)$_2$]•0.43H_2O (***Eu-1***). The dimer was synthesized according to the general procedure using 94.7 mg $EuCl_3$•6H_2O (258 μmol), 58.8 mg terpy (252 μmol), and 100.2 mg 2-HTC (782 μmol). Large colorless rhombus-shaped crystals were collected by filtration, washed with water, dried, and collected in an 86% yield (171 mg). Elemental Analysis: Calcd. for $C_{60}H_{44.86}N_6O_{14.43}S_6Eu_2$: C, 45.67; H, 2.87; N, 5.33. Found: C, 45.71; H, 2.73; N, 5.25.

[Gd_2(terpy)$_2$(TC)$_6$(H_2O)$_2$]•0.37H_2O (***Gd-1***). The dimer was synthesized according to the general procedure using 45.7 mg Gd_2O_3 (126 μmol), 61.9 mg terpy (265 μmol), and 98.5 mg 2-HTC (769 μmol). Small colorless rhombus-shaped crystals were collected by filtration, washed with water, dried, and collected in a 71% yield (142 mg). Elemental Analysis: Calcd. for $C_{60}H_{44.74}N_6O_{14.37}S_6Gd_2$: C, 45.42; H, 2.84; N, 5.30. Found: C, 45.36; H, 2.80; N, 5.23.

[Tb_2(terpy)$_2$(TC)$_6$(H_2O)$_2$]•0.34H_2O (***Tb-1***). The dimer was synthesized according to the general procedure using 95.5 mg $TbCl_3$•6H_2O (256 μmol), 57.9 mg terpy (248 μmol), and 96.8 mg 2-HTC (755 μmol). Large colorless rhombus-shaped crystals were collected by filtration,

washed with water, dried, and collected in a 77% yield (152 mg). Elemental Analysis: Calcd. for $C_{60}H_{44.68}N_6O_{14.34}S_6Tb_2$: C, 45.33; H, 2.84; N, 5.29. Found: C, 45.28; H, 2.74; N, 5.22.

[Dy_2(terpy)$_2$(TC)$_6$(H_2O)$_2$]•0.30H_2O (***Dy-1***). The dimer was synthesized according to the general procedure using 101.4 mg $DyCl_3$•6H_2O (269 μmol), 60.8 mg terpy (260 μmol), and 99.8 mg 2-HTC (779 μmol). Small colorless rhombus-shaped crystals were collected by filtration, washed with water, dried, and collected in a 71% yield (148 mg). Elemental Analysis: Calcd. for $C_{60}H_{44.60}N_6O_{14.30}S_6Dy_2$: C, 45.16; H, 2.82; N, 5.27. Found: C, 45.13; H, 2.72; N, 5.20.

[Ho_2(terpy)$_2$*(TC)$_6$*(H_2O)$_2$*]•0.30H_2O* (***Ho-1***). The dimer was synthesized according to the general procedure using 96.3 mg $HoCl_3$•6H_2O (254 μmol), 59.5 mg terpy (255 μmol), and 99.8 mg 2-HTC (771 μmol). Small pink rhombus-shaped crystals were manually separated from the bulk product and used directly for single-crystal X-ray diffraction studies. Subsequent analysis of the bulk reaction product via powder X-ray diffraction showed that **Ho-1** was not the sole reaction product; the second phase was later identified to be isomorphous with **Er-3**.

[Ho_2(terpy)$_2$(TC)$_5$(H_2O)$_2$]TC (***Ho-2***). The dimer was synthesized according to the general procedure using 46.7 mg Ho_2O_3 (124 μmol), 60.0 mg terpy (257 μmol), and 98.6 mg 2-HTC (769 μmol). Large pale pink block crystals were collected by filtration, washed with water, dried, and collected in a 68% yield (134 mg). Elemental Analysis: Calcd. for $C_{60}H_{44}N_6O_{14}S_6Ho_2$: C, 45.10; H, 2.79; N, 5.26. Found: C, 45.38; H, 2.63; N, 4.99.

[(Er(terpy)(TC)$_3$(H_2O)] (***Er-3***). The monomer was synthesized according to the general procedure using 47.8 mg Er_2O_3 (125 μmol), 58.6 mg terpy (251 μmol), and 99.5 mg 2-HTC (776 μmol). Large colorless rods were collected by filtration, washed with water, dried, and collected in an 84% yield (168 mg). Elemental Analysis: Calcd. for $C_{30}H_{22}N_3O_7S_3Er$: C, 45.04; H, 2.77; N, 5.25. Found: C, 45.12; H, 2.85; N, 5.35.

[Tm(terpy)(TC)$_3$(H_2O)] (***Tm-4***). The monomer was synthesized according to the general procedure using 48.2 mg Tm_2O_3 (125 μmol), 59.0 mg terpy (253 μmol), and 98.3 mg 2-HTC (767 μmol). Small colorless rods were collected by filtration, washed with water, dried, and collected in a 59% yield (118 mg). Elemental Analysis: Calcd. for $C_{30}H_{22}N_3O_7S_3Tm$: C, 44.95; H, 2.77; N, 5.24. Found: C, 44.82; H, 2.85; N, 5.20.

[Yb(terpy)(TC)$_3$(H_2O)] (***Yb-4***). The monomer was synthesized according to the general procedure using 106.2 mg $YbCl_3$•6H_2O (274 μmol), 58.8 mg terpy (252 μmol), and 98.5 mg 2-HTC (769 μmol). Large colorless rods were collected by filtration, washed with water, dried, and collected in a 72% yield (146 mg). Elemental Analysis: Calcd. for $C_{30}H_{22}N_3O_7S_3Yb$: C, 44.72; H, 2.75; N, 5.22. Found: C, 44.62; H, 2.70; N, 5.20.

[Lu(terpy)(TC)$_3$(H_2O)] (***Lu-4***). The monomer was synthesized according to the general procedure using 102.7 mg $LuCl_3$•6H_2O (264 μmol), 61.2 mg terpy (262 μmol), and 100.6 mg 2-HTC (785 μmol). Small colorless rods were collected by filtration, washed with water, dried, and collected in a 64% yield (135 mg). Elemental Analysis: Calcd. for $C_{30}H_{22}N_3O_7S_3Lu$: C, 44.61; H, 2.75; N, 5.20. Found: C, 44.38; H, 2.67; N, 5.13.

Crystallographic Refinement Details

Single crystals of each compound were mounted under paratone oil on a Mitegen micromount and immediately placed in a cold nitrogen stream prior to data collection. All single crystal data were collected on a Bruker D8 Quest equipped with a Photon100 CMOS detector and a Mo ImS source. Data were collected using a combination of phi and omega scans and integrated with the Bruker SAINT program. Structure solutions were performed using the SHELXTL software suite. Intensities were corrected for Lorentz and polarization effects and an empirical absorption correction was applied using SADABS v2014/4. Non-hydrogen atoms were refined with anisotropic thermal parameters and hydrogen atoms were included in idealized positions unless otherwise noted. The thiophene ring portion of the TC ligand was disordered over two orientations, and the like S-C and C-C bonds were restrained to be similar. Outer coordination sphere water molecules were partially occupied and refined using as free variable commands. The water H atoms were located in the difference map and the O-H distance was restrained to 0.86(2) Å. These H atoms refine to good hydrogen bonding positions. Further comments on disorder models:

$[(terpy)La(TC)_2(\mu\text{-}TC)(H_2O)]_2 \bullet 0.79H_2O$ (**La-1**).
The thiophene ring portion of all three coordinated TC ligands is disordered over two orientations. The like S-C and C-C bonds have been restrained to be similar. The *ipso*-carbon of disordered TC rings were constrained using EADP and EXYZ commands. The unbound water molecule is partially occupied within the lattice structure and was refined using a free variable to determine the percent occupancy. Similar displacement amplitudes were imposed on disordered sites overlapping by less than the sum of van der Waals radii. Rigid-bond restraints were also imposed on the molecule. The water H atoms were located in the difference map and the O-H distance was restrained to be 0.86Å. These H atoms refine to good hydrogen bonding positions.

$[(terpy)Ce(TC)_2(\mu\text{-}TC)(H_2O)]_2 \bullet 0.69H_2O$ (**Ce-1**).
The thiophene ring portion of all three coordinated TC ligands is disordered over two orientations. The like S-C and C-C bonds have been restrained to be similar. The unbound water molecule is partially occupied within the lattice structure and was refined using a free variable to determine the percent occupancy. Similar displacement amplitudes were imposed on disordered sites overlapping by less than the sum of van der Waals radii. Rigid-bond restraints were also imposed on the molecule. The water H atoms were located in the difference map and the O-H distance was restrained to be 0.86Å. These H atoms refine to good hydrogen bonding positions.

$[(terpy)Pr(TC)_2(\mu\text{-}TC)(H_2O)]_2 \bullet 0.64H_2O$ (**Pr-1**).
The thiophene ring portion of all three coordinated TC ligands is disordered over two orientations. The like S-C and C-C bonds have been restrained to be similar. The *ipso*-carbon of the S2 and S3 TC rings were constrained using EADP and EXYZ commands. The unbound water molecule is partially occupied within the lattice structure and was refined using a free variable to determine the percent occupancy. Similar displacement amplitudes were imposed on disordered sites overlapping by less than the sum of van der Waals radii. Rigid-bond restraints were also imposed on the molecule. The water H atoms were located in the difference map and the O-H distance was restrained to be 0.86Å. These H atoms refine to good hydrogen bonding positions.

[(terpy)Nd(TC)$_2$(μ-TC)(H$_2$O)]$_2$•0.63H$_2$O (**Nd-1**).
The thiophene ring portion of all three coordinated TC ligands is disordered over two orientations. The like S-C and C-C bonds have been restrained to be similar. The *ipso*-carbon of the S2 and S3 TC rings were constrained using EADP and EXYZ commands. The unbound water molecule is partially occupied within the lattice structure and was refined using a free variable to determine the percent occupancy. Similar displacement amplitudes were imposed on disordered sites overlapping by less than the sum of van der Waals radii. Rigid-bond restraints were also imposed on the molecule. The water H atoms of the bound water molecule were located in the difference map and the O-H distance was restrained to be 0.86Å. These H atoms refine to good hydrogen bonding positions. The H atoms of the lattice water could not be located on the difference map, and were thus omitted.

[(terpy)Sm(TC)$_2$(μ-TC)(H$_2$O)]$_2$•0.42H$_2$O (**Sm-1**).
The thiophene ring portion of all three coordinated TC ligands is disordered over two orientations. The like S-C and C-C bonds have been restrained to be similar. The unbound water molecule is partially occupied within the lattice structure and was refined using a free variable to determine the percent occupancy. Similar displacement amplitudes were imposed on disordered sites overlapping by less than the sum of van der Waals radii. The water H atoms were located in the difference map and the O-H distance was restrained to be 0.86Å. These H atoms refine to good hydrogen bonding positions.

[(terpy)Eu(TC)$_2$(μ-TC)(H$_2$O)]$_2$•0.43H$_2$O (**Eu-1**).
The thiophene ring portion of all three coordinated TC ligands is disordered over two orientations. The like S-C and C-C bonds have been restrained to be similar. The unbound water molecule is partially occupied within the lattice structure and was refined using a free variable to determine the percent occupancy. Similar displacement amplitudes were imposed on disordered sites overlapping by less than the sum of van der Waals radii. Rigid-bond restraints were also imposed on the molecule. For atoms C20A, C28A, and S1A, ISOR commands were used to restrain the anisotropic displacement parameters to be more isotropic. The water H atoms were located in the difference map and the O-H distance was restrained to be 0.86Å. These H atoms refine to good hydrogen bonding positions.

[(terpy)Gd(TC)$_2$(μ-TC)(H$_2$O)]$_2$•0.37H$_2$O (**Gd-1**).
The thiophene ring portion of all three coordinated TC ligands is disordered over two orientations. The like S-C and C-C bonds have been restrained to be similar. The unbound water molecule is partially occupied within the lattice structure and was refined using a free variable to determine the percent occupancy. Similar displacement amplitudes were imposed on disordered sites overlapping by less than the sum of van der Waals radii. Rigid-bond restraints were also imposed on the molecule. The water H atoms were located in the difference map and the O-H distance was restrained to be 0.86Å. These H atoms refine to good hydrogen bonding positions.

[(terpy)Tb(TC)$_2$(μ-TC)(H$_2$O)]$_2$•0.34H$_2$O (**Tb-1**).
The thiophene ring portion of all three coordinated TC ligands is disordered over two orientations. The like S-C and C-C bonds have been restrained to be similar. The unbound water molecule is partially occupied within the lattice structure and was refined using a free variable to determine the percent occupancy. Similar displacement amplitudes were imposed on disordered

sites overlapping by less than the sum of van der Waals radii. The water H atoms were located in the difference map and the O-H distance was restrained to be 0.86Å. These H atoms refine to good hydrogen bonding positions.

[(terpy)Dy(TC)$_2$(μ-TC)(H$_2$O)]$_2$•0.30H$_2$O (**Dy-1**).
The thiophene ring portion of all three coordinated TC ligands is disordered over two orientations. The like S-C and C-C bonds have been restrained to be similar. The unbound water molecule is partially occupied within the lattice structure and was refined using a free variable to determine the percent occupancy. Similar displacement amplitudes were imposed on disordered sites overlapping by less than the sum of van der Waals radii. Rigid-bond restraints were also imposed on the molecule. The water H atoms were located in the difference map and the O-H distance was restrained to be 0.86Å. These H atoms refine to good hydrogen bonding positions.

[(terpy)Ho(TC)$_2$(μ-TC)(H$_2$O)]$_2$•0.32H$_2$O (**Ho-1**).
The thiophene ring portion of all three coordinated TC ligands is disordered over two orientations. The like S-C and C-C bonds have been restrained to be similar. The unbound water molecule is partially occupied within the lattice structure and was refined using a free variable to determine the percent occupancy. Similar displacement amplitudes were imposed on disordered sites overlapping by less than the sum of van der Waals radii. Rigid-bond restraints were also imposed on the molecule. For the lattice water oxygen (O8), an ISOR command was imposed to restrain the anisotropic displacement parameters to be more isotropic. The water H atoms were located in the difference map and the O-H distance was restrained to be 0.86Å. These H atoms refine to good hydrogen bonding positions.

[(terpy)Ho(TC)$_2$(μ-TC)$_2$(TC)(H$_2$O)$_2$Ho(terpy)]TC (**Ho-2**).
The thiophene ring portion of all six coordinated TC ligands is disordered over two orientations. The like S-C and C-C bonds have been restrained to be similar. The *ipso*-carbon of the S1 through S5 TC rings were constrained using EADP and EXYZ commands. Similar displacement amplitudes were imposed on disordered sites overlapping by less than the sum of van der Waals radii. Rigid-bond restraints were also imposed on the molecule. The water H atoms were located in the difference map and the O-H distance was restrained to be 0.86Å. These H atoms refine to good hydrogen bonding positions.

[(terpy)Er(TC)$_3$(H$_2$O)] (**Er-3**).
The thiophene ring portion of all three coordinated TC ligands is disordered over two orientations. The like S-C and C-C bonds have been restrained to be similar. Similar displacement amplitudes were imposed on disordered sites overlapping by less than the sum of van der Waals radii. Rigid-bond restraints were also imposed on the molecule. The water H atoms were located in the difference map and the O-H distance was restrained to be 0.86Å. These H atoms refine to good hydrogen bonding positions.

[(terpy)Tm(TC)$_3$(H$_2$O)] (**Tm-3**).
The thiophene ring portion of all three coordinated TC ligands is disordered over two orientations. The like S-C and C-C bonds have been restrained to be similar. The *ipso*-carbon of all TC rings were constrained using EADP and EXYZ commands. Similar displacement amplitudes were imposed on disordered sites overlapping by less than the sum of van der Waals

radii. Rigid-bond restraints were also imposed on the molecule. For the TC sulfur S2B, an ISOR command was imposed to restrain the anisotropic displacement parameters to be more isotropic. The water H atoms were located in the difference map and the O-H distance was restrained to be 0.86Å. These H atoms refine to good hydrogen bonding positions.

[(terpy)Yb$(TC)_3(H_2O)$] (**Yb-3**).
The thiophene ring portion of all three coordinated TC ligands is disordered over two orientations. The like S-C and C-C bonds have been restrained to be similar. Similar displacement amplitudes were imposed on disordered sites overlapping by less than the sum of van der Waals radii. Rigid-bond restraints were also imposed on the molecule. The water H atoms were located in the difference map and the O-H distance was restrained to be 0.86Å. These H atoms refine to good hydrogen bonding positions.

[(terpy)Lu$(TC)_3(H_2O)$] (**Lu-3**).
The thiophene ring portion of all three coordinated TC ligands is disordered over two orientations. The like S-C and C-C bonds have been restrained to be similar. Similar displacement amplitudes were imposed on disordered sites overlapping by less than the sum of van der Waals radii. Rigid-bond restraints were also imposed on the molecule. For the TC atoms S1A and C18, ISOR commands were used to restrain the anisotropic displacement parameters to be more isotropic. The water H atoms were located in the difference map and the O-H distance was restrained to be 0.86Å. These H atoms refine to good hydrogen bonding positions.

Solid-State Crystal Structures

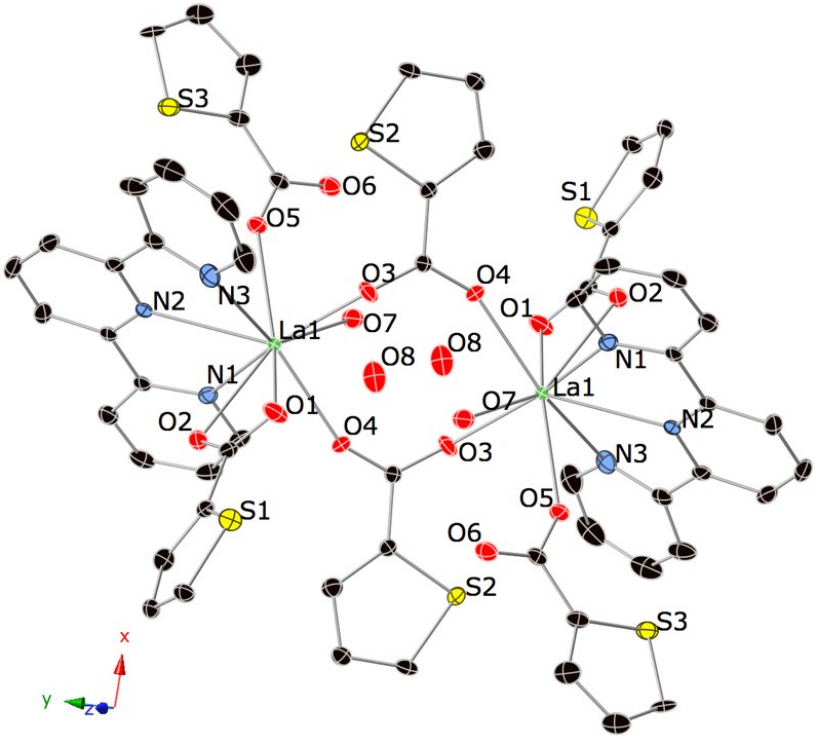

Figure S1. Thermal ellipsoid plot of **La-1**; thermal ellipsoids are shown at 50% probability level. Color code: La, green; S, yellow; O, red; N, light blue; C, black.

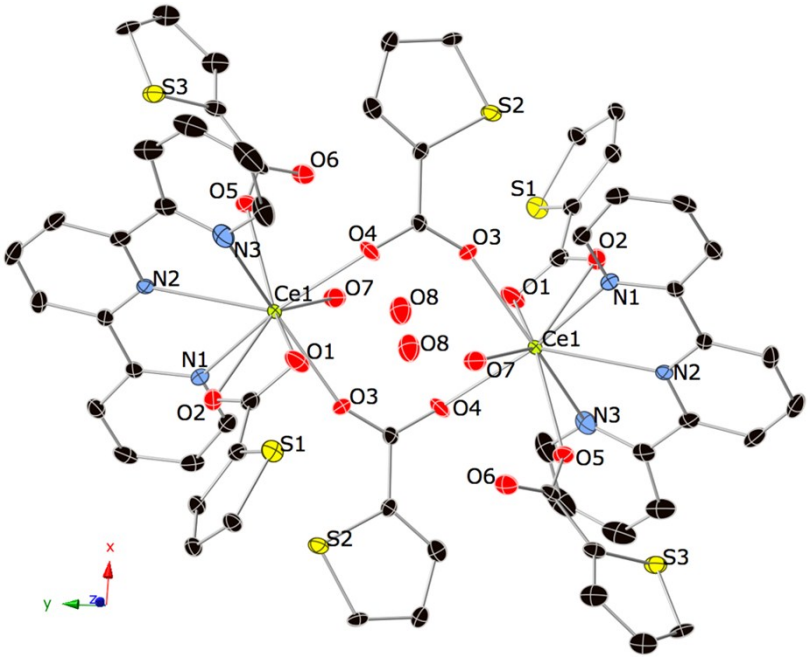

Figure S2. Thermal ellipsoid plot of **Ce-1**; thermal ellipsoids are shown at 50% probability level. Color code: Ce, lime green; S, yellow; O, red; N, light blue; C, black.

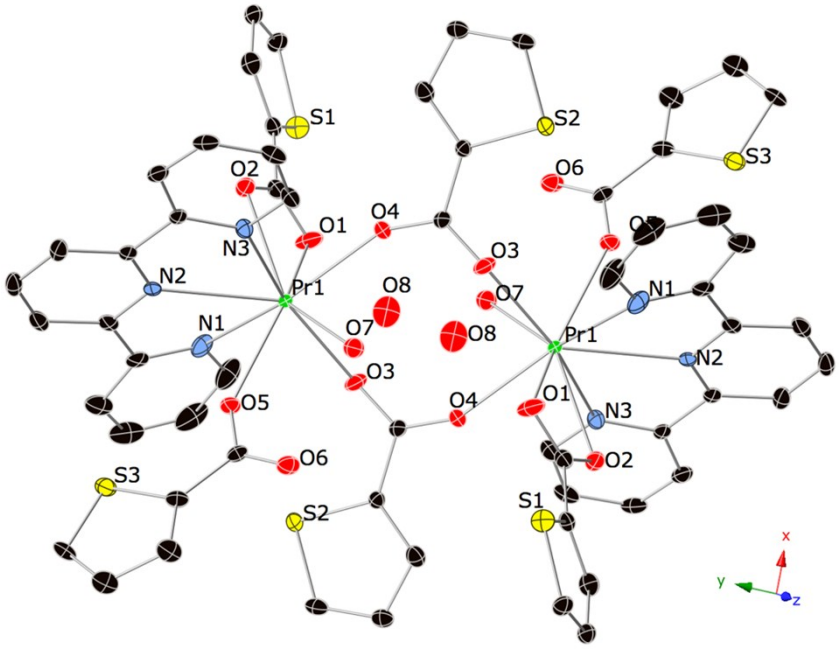

Figure S 3. Thermal ellipsoid plot of **Pr-1**; thermal ellipsoids are shown at 50% probability level. Color code: Pr, green; S, yellow; O, red; N, light blue; C, black.

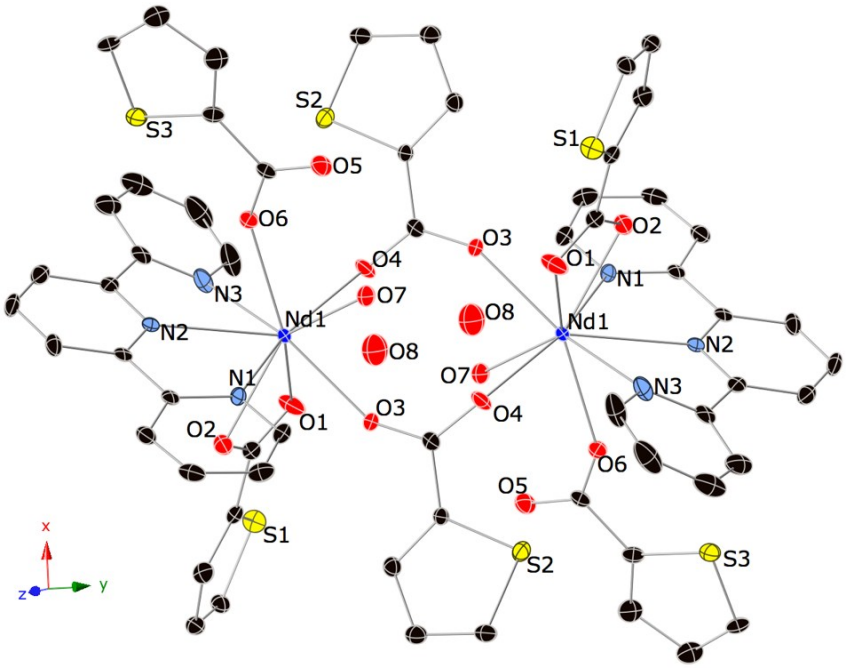

Figure S 4. Thermal ellipsoid plot of **Nd-1**; thermal ellipsoids are shown at 50% probability level. Color code: Nd, dark blue; S, yellow; O, red; N, light blue; C, black.

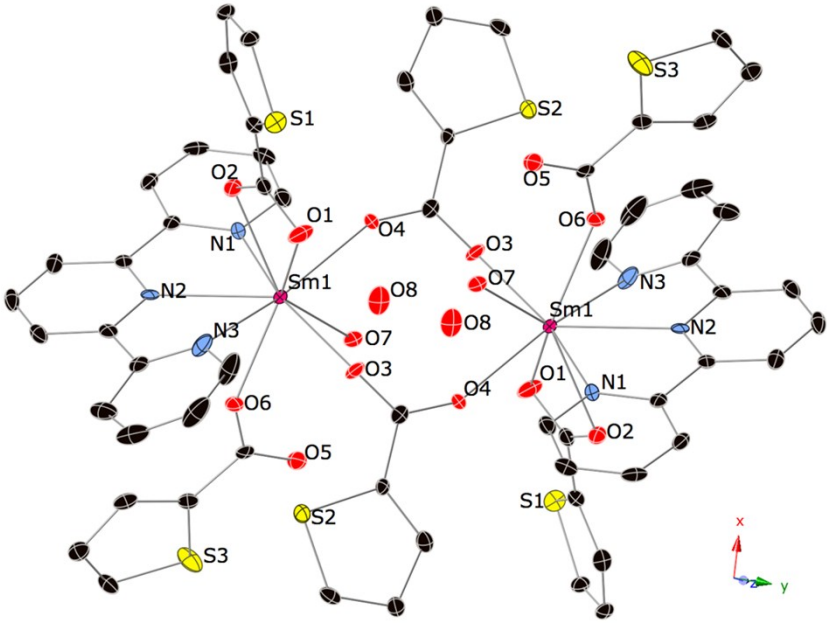

Figure S 5. Thermal ellipsoid plot of **Sm-1**; thermal ellipsoids are shown at 50% probability level. Color code: Sm, pink; S, yellow; O, red; N, light blue; C, black.

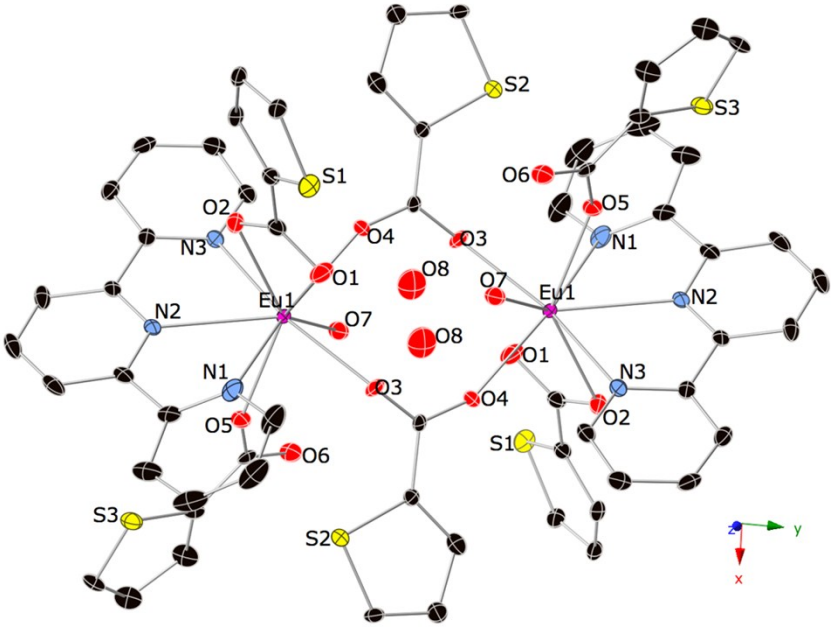

Figure S 6. Thermal ellipsoid plot of **Eu-1**; thermal ellipsoids are shown at 50% probability level. Color code: Eu, fuchsia; S, yellow; O, red; N, light blue; C, black.

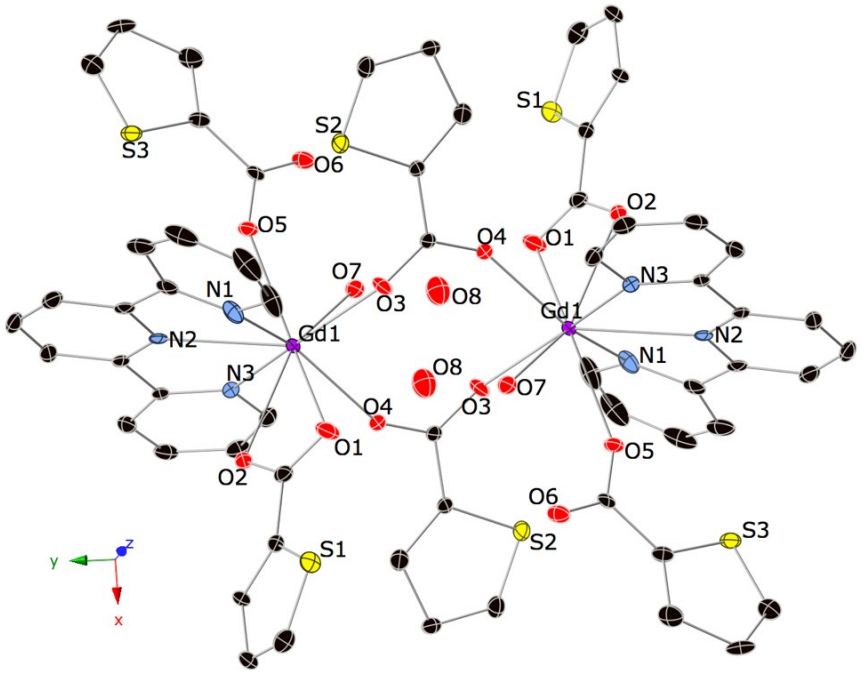

Figure S 7. Thermal ellipsoid plot of **Gd-1**; thermal ellipsoids are shown at 50% probability level. Color code: Gd, purple; S, yellow; O, red; N, light blue; C, black.

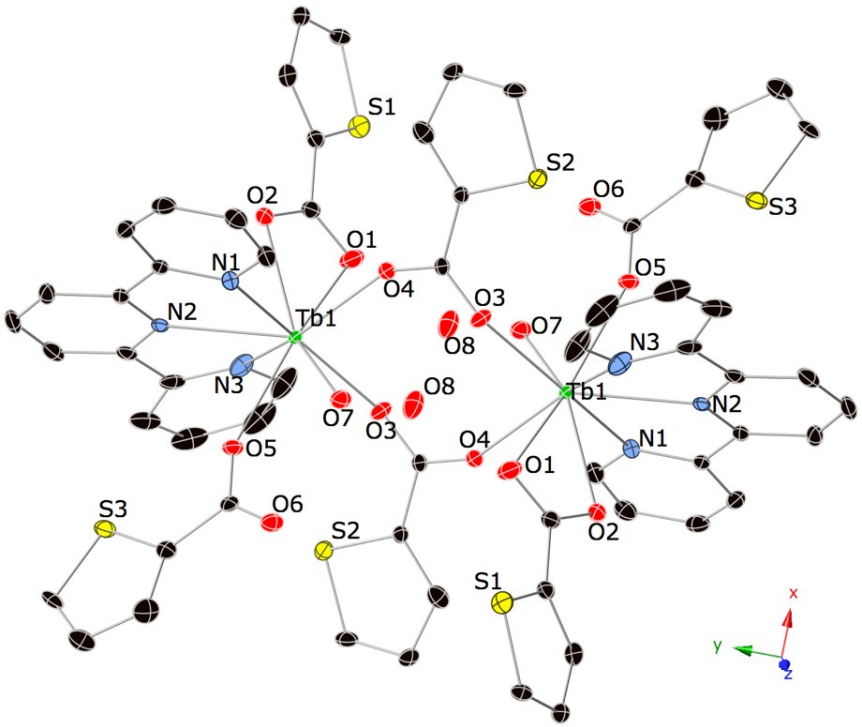

Figure S 8. Thermal ellipsoid plot of **Tb-1**; thermal ellipsoids are shown at 50% probability level. Color code: Tb, green; S, yellow; O, red; N, light blue; C, black.

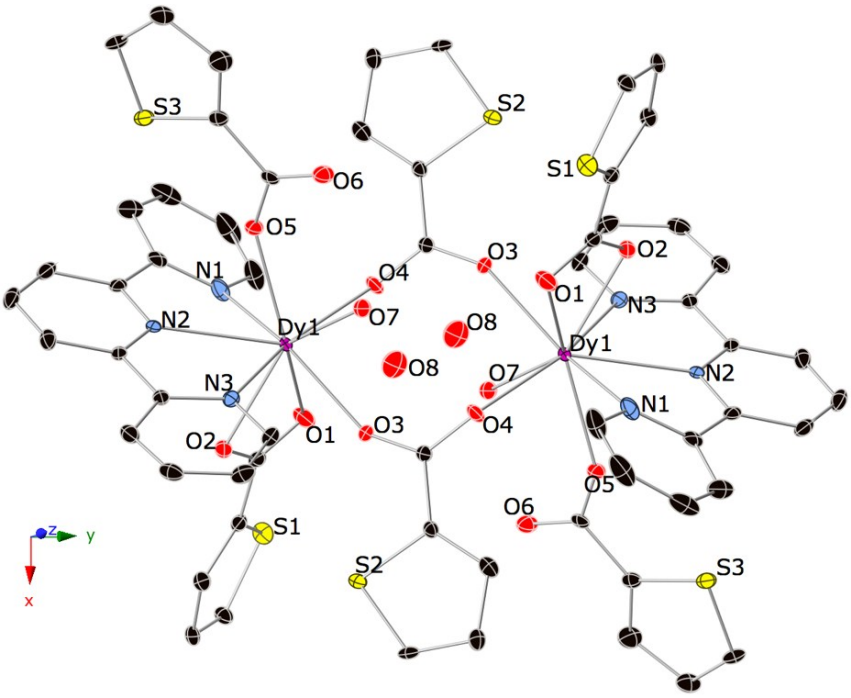

Figure S 9. Thermal ellipsoid plot of **Dy-1**; thermal ellipsoids are shown at 50% probability level. Color code: Dy, fuchsia; S, yellow; O, red; N, light blue; C, black.

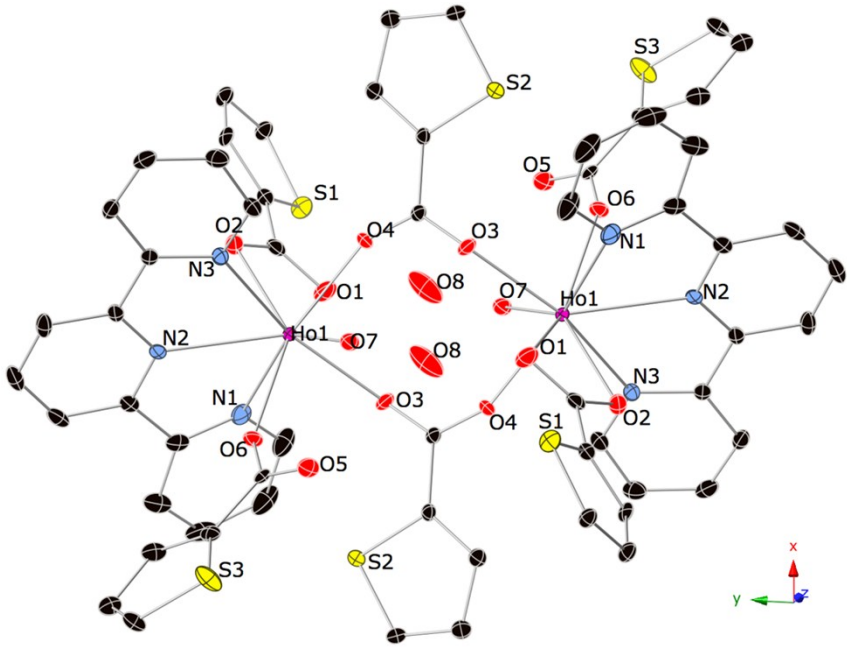

Figure S 10. Thermal ellipsoid plot of **Ho-1**; thermal ellipsoids are shown at 50% probability level. Color code: Ho, pink; S, yellow; O, red; N, light blue; C, black.

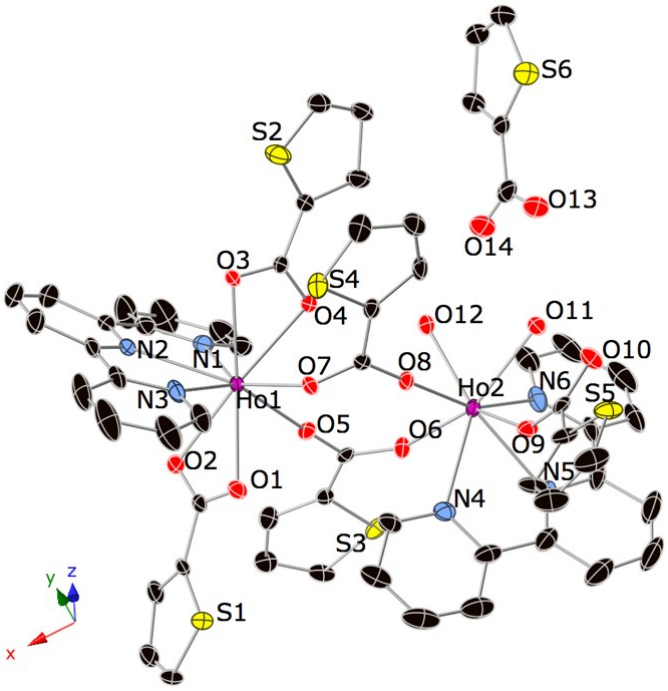

Figure S 11. Thermal ellipsoid plot of **Ho-2**; thermal ellipsoids are shown at 50% probability level. Color code: Ho, fuchsia; S, yellow; O, red; N, light blue; C, black.

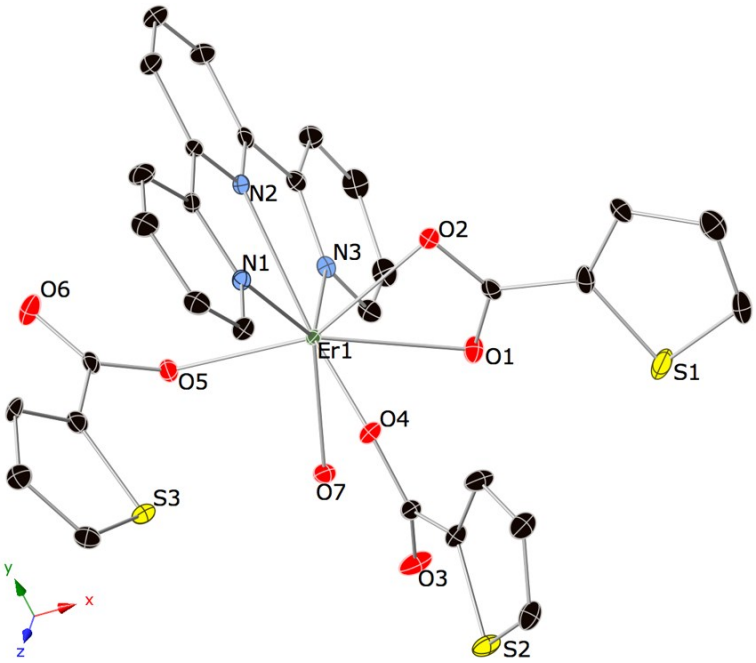

Figure S 12. Thermal ellipsoid plot of **Er-3**; thermal ellipsoids are shown at 50% probability level. Color code: Er, green; S, yellow; O, red; N, light blue; C, black.

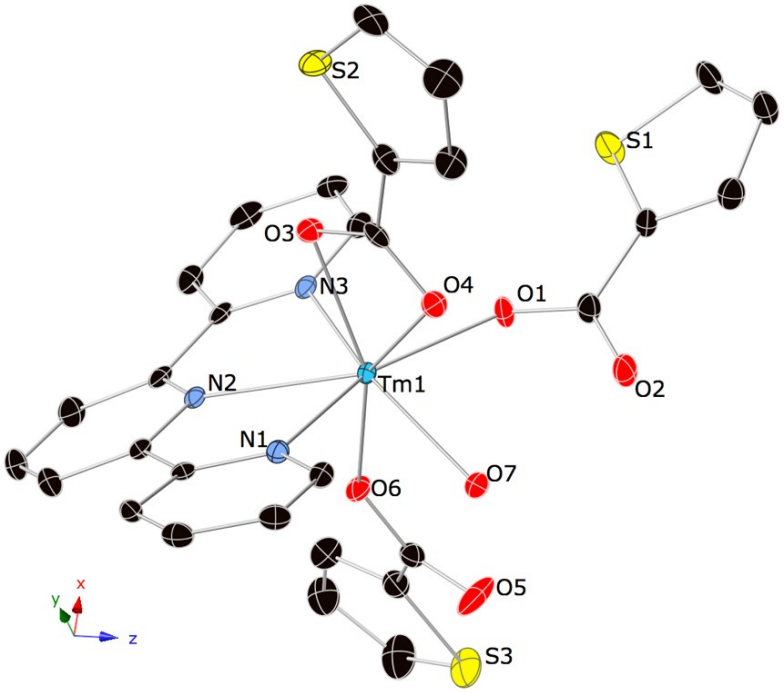

Figure S 13. Thermal ellipsoid plot of **Tm-4**; thermal ellipsoids are shown at 50% probability level. Color code: Tm, blue; S, yellow; O, red; N, light blue; C, black.

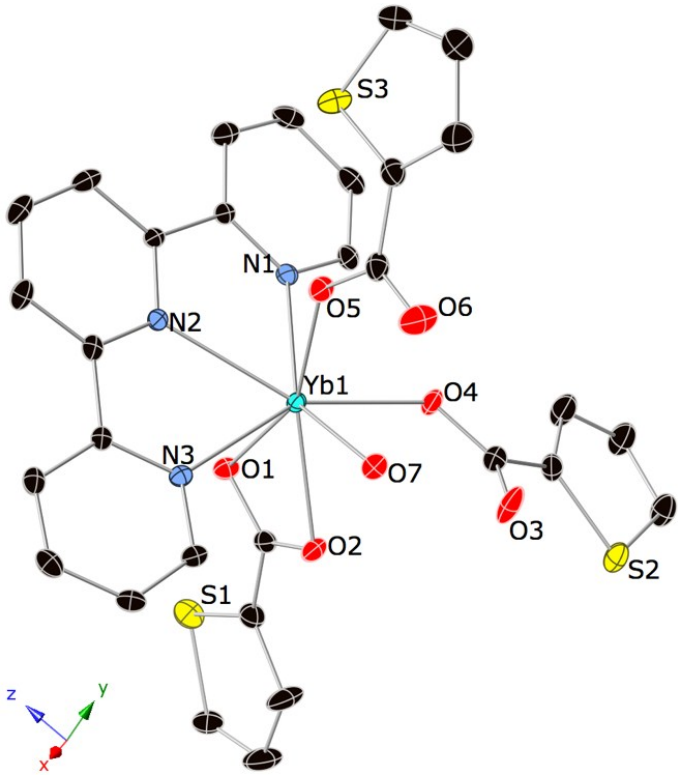

Figure S 14. Thermal ellipsoid plot of **Yb-4**; thermal ellipsoids are shown at 50% probability level. Color code: Yb, teal; S, yellow; O, red; N, light blue; C, black.

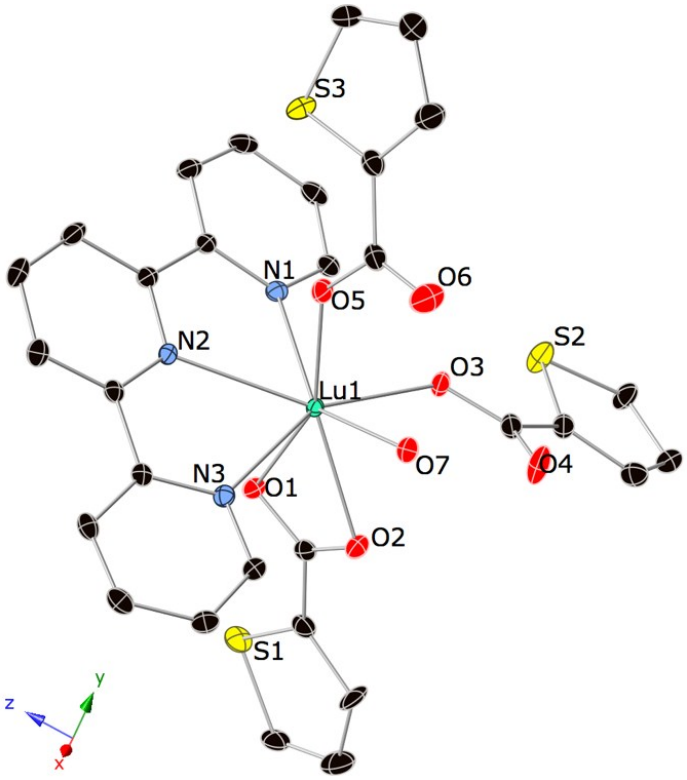

Figure S 15. Thermal ellipsoid plot of **Lu-4**; thermal ellipsoids are shown at 50% probability level. Color code: Lu, teal; S, yellow; O, red; N, light blue; C, black.

Powder X-Ray Diffraction Patterns

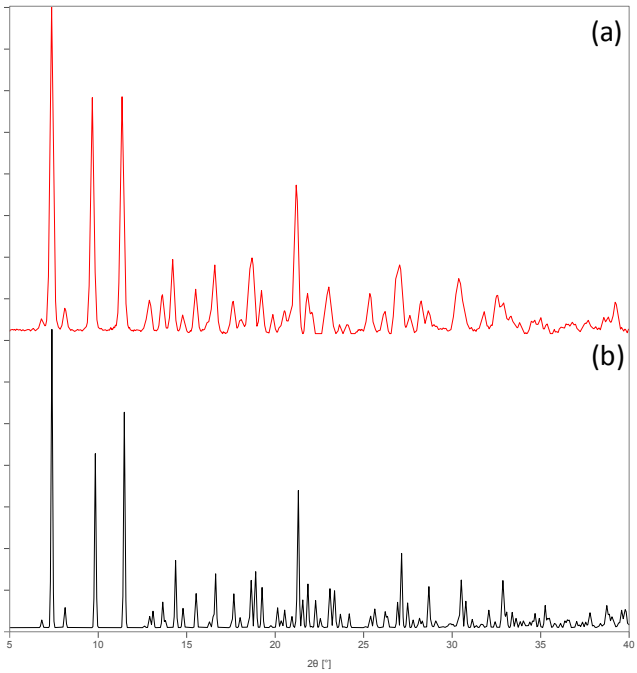

Figure S 16. Experimental (a) and calculated (b) PXRD pattern of **La-1**. Experimental diffraction patterns were acquired using Cu Kα radiation.

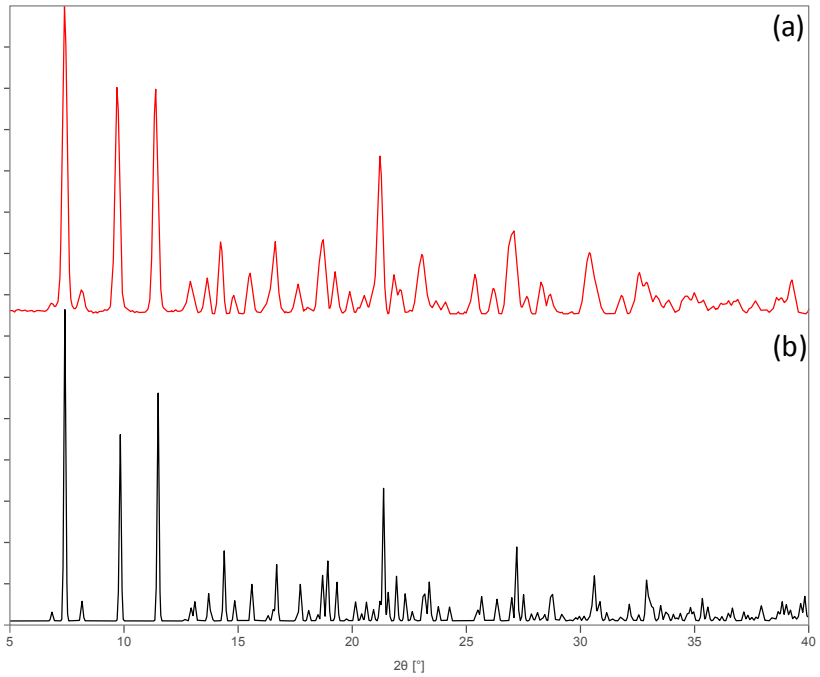

Figure S 17. Experimental (a) and calculated (b) PXRD pattern of **Ce-1**. Experimental diffraction patterns were acquired using Cu Kα radiation.

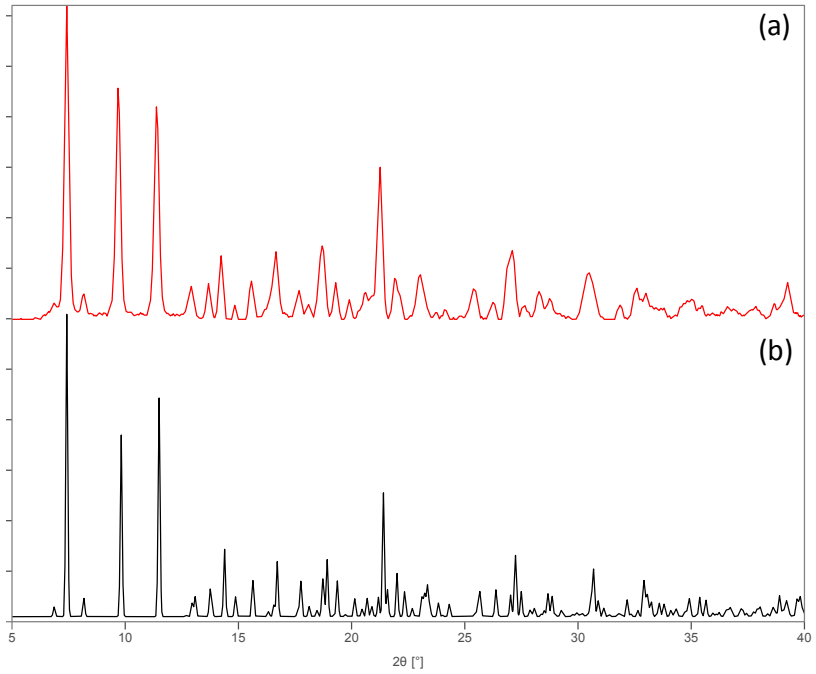

Figure S 18. Experimental (a) and calculated (b) PXRD pattern of **Pr-1**. Experimental diffraction patterns were acquired using Cu Kα radiation.

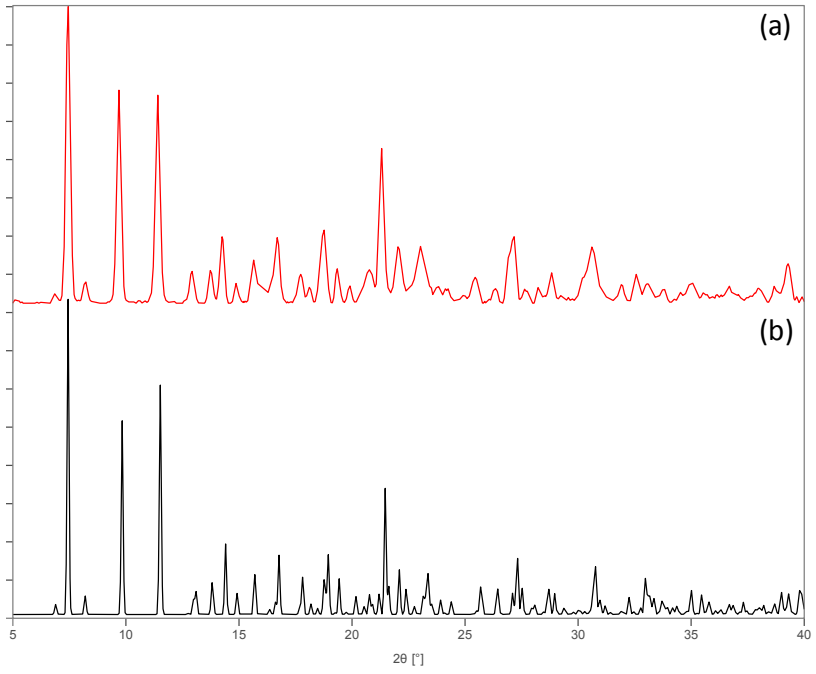

Figure S 19. Experimental (a) and calculated (b) PXRD pattern of **Nd-1**. Experimental diffraction patterns were acquired using Cu Kα radiation.

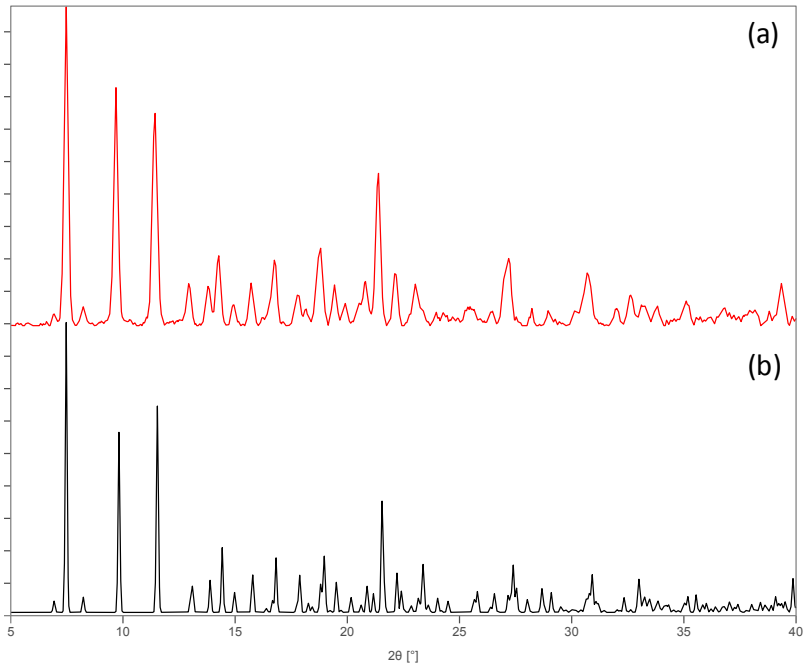

Figure S 20. Experimental (a) and calculated (b) PXRD pattern of **Sm-1**. Experimental diffraction patterns were acquired using Cu Kα radiation.

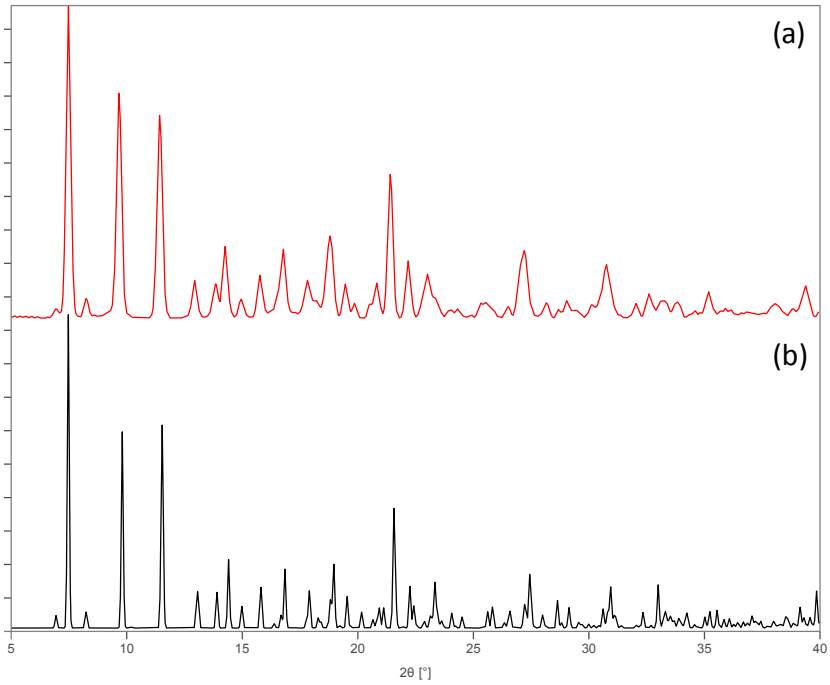

Figure S 21. Experimental (a) and calculated (b) PXRD pattern of **Eu-1**. Experimental diffraction patterns were acquired using Cu Kα radiation.

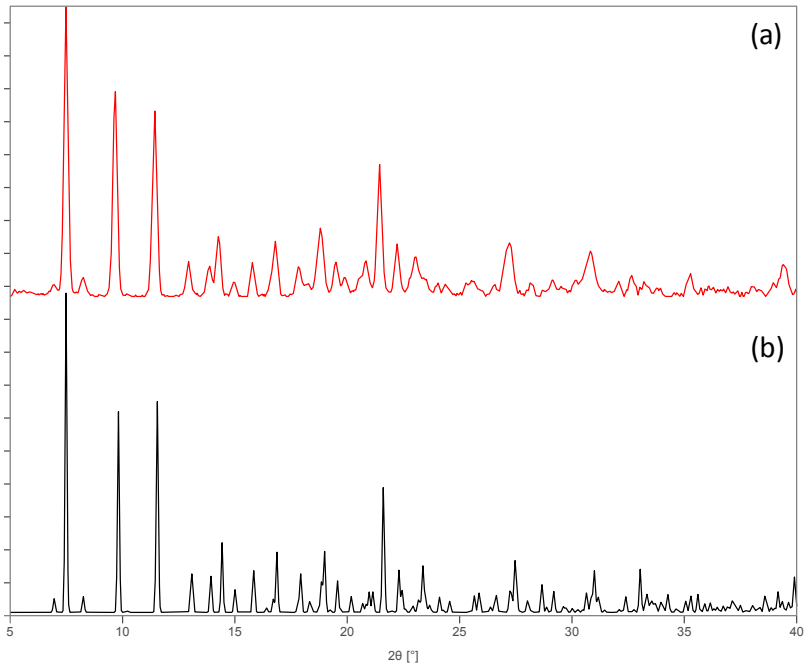

Figure S 22. Experimental (a) and calculated (b) PXRD pattern of **Gd-1**. Experimental diffraction patterns were acquired using Cu Kα radiation.

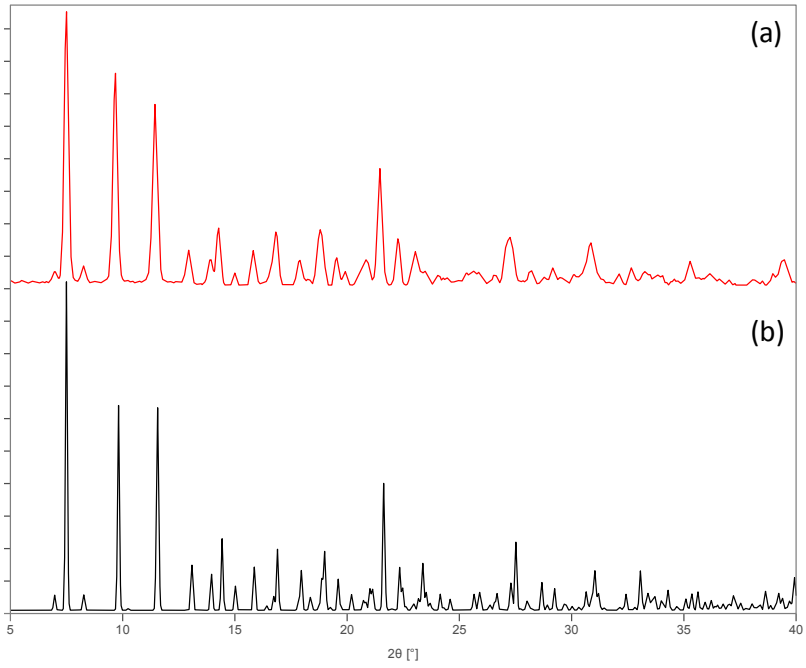

Figure S 23. Experimental (a) and calculated (b) PXRD pattern of **Tb-1**. Experimental diffraction patterns were acquired using Cu Kα radiation.

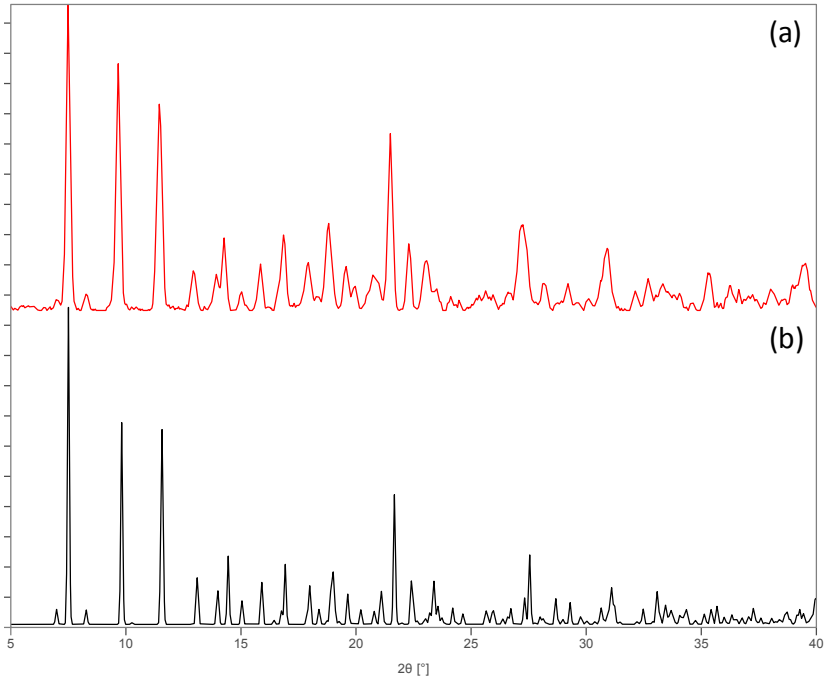

Figure S 24. Experimental (a) and calculated (b) PXRD pattern of **Dy-1**. Experimental diffraction patterns were acquired using Cu Kα radiation.

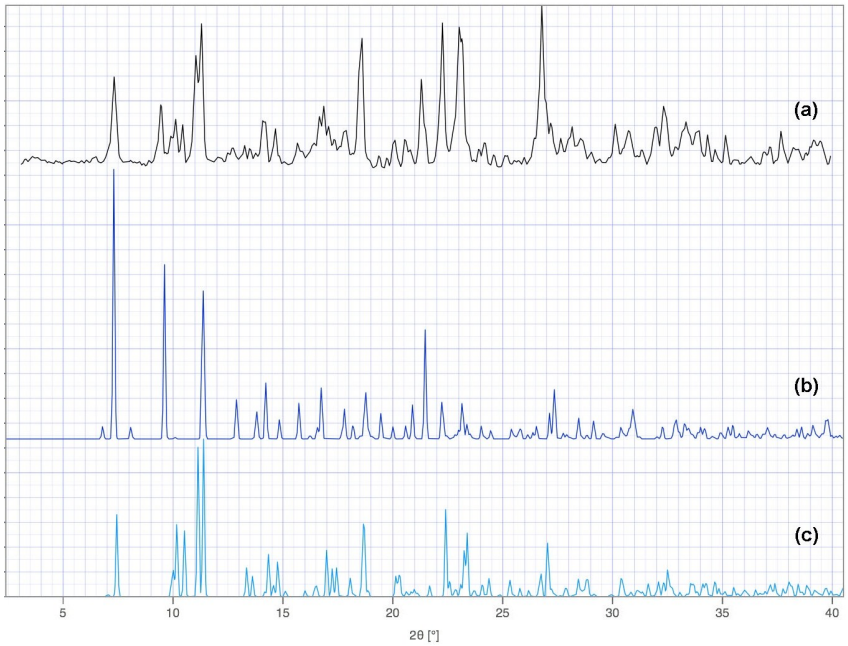

Figure S 25. (a) Experimental powder pattern obtained for bulk reaction product from $HoCl_3$ reaction. Calculated pattern for (b) **Ho-1** and (c) **Er-3.** Note that we were unable to isolate single crystals of **Ho-3.** All PXRD data was collected using Cu Kα radiation.

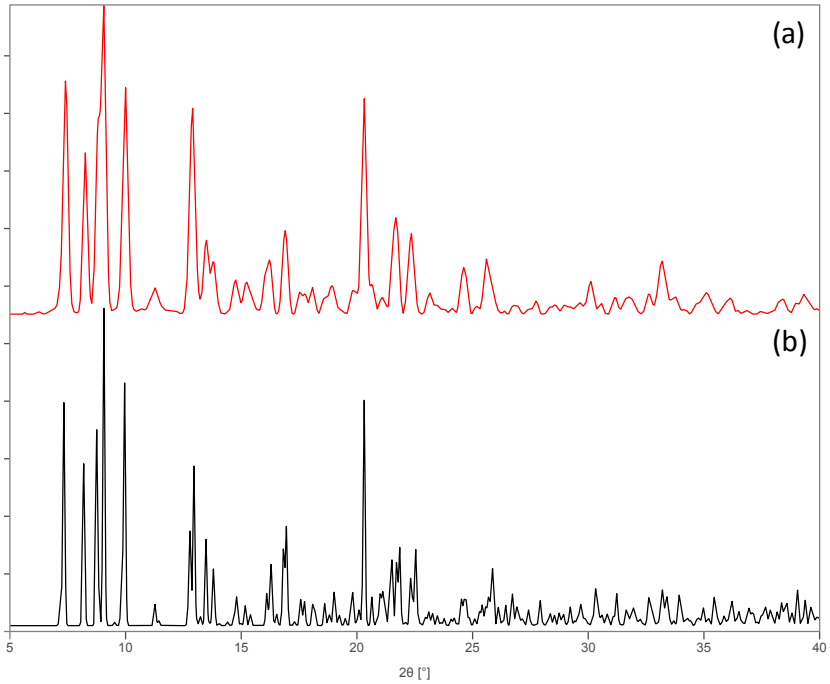

Figure S 26. (a) Experimental powder pattern obtained for bulk reaction product prepared from Ho_2O_3 starting material. (b) Calculated pattern of **Ho-2**. Experimental PXRD patterns were acquired using Cu Kα radiation.

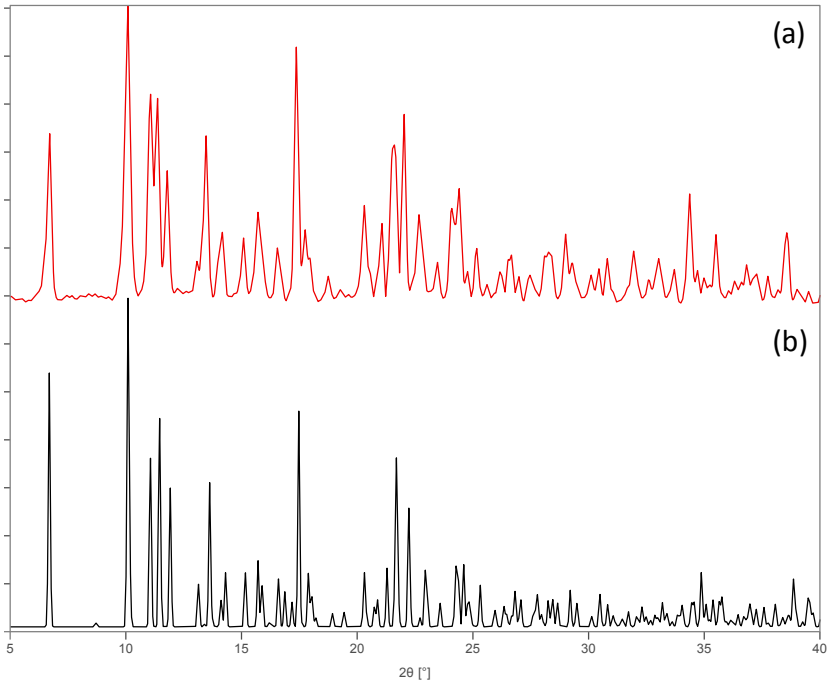

Figure S 27. Experimental (a) and calculated (b) PXRD pattern of **Er-3**. Experimental diffraction patterns were acquired using Cu Kα radiation.

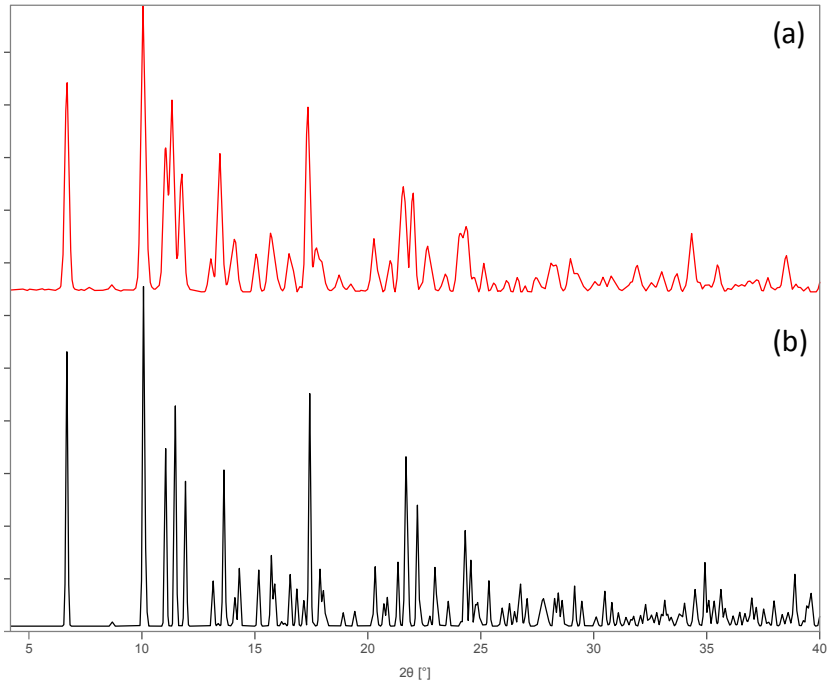

Figure S 28. Experimental (a) and calculated (b) PXRD pattern of **Tm-3**. Experimental diffraction patterns were acquired using Cu Kα radiation.

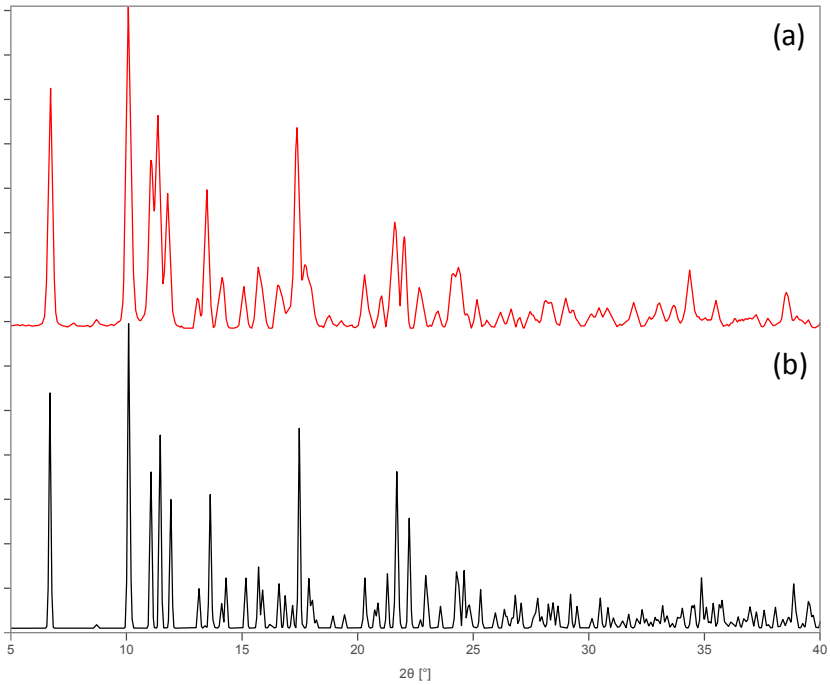

Figure S 29. Experimental (a) and calculated (b) PXRD pattern of **Yb-3**. Experimental diffraction patterns were acquired using Cu Kα radiation.

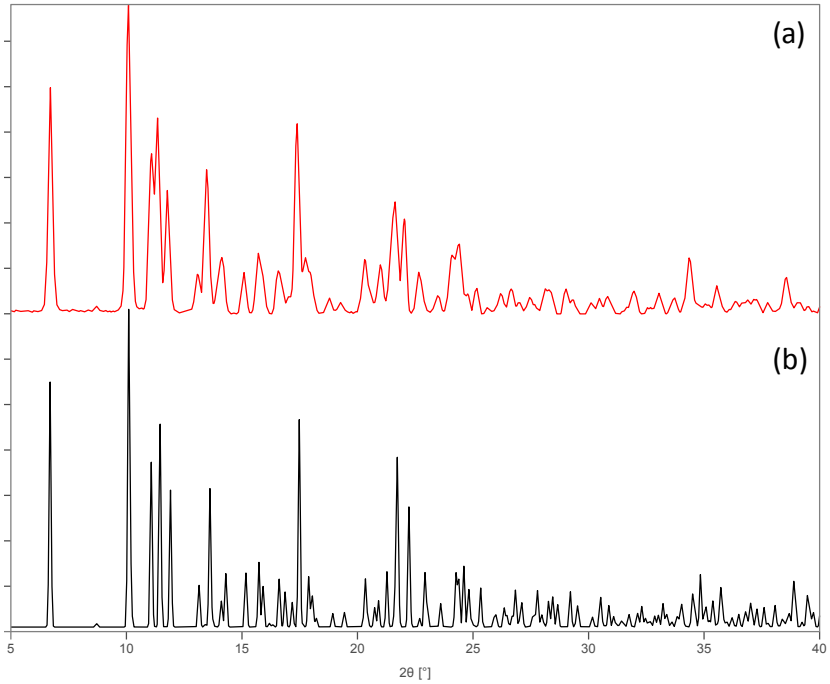

Figure S 30. Experimental (a) and calculated (b) PXRD pattern of **Lu-3**. Experimental diffraction patterns were acquired using Cu Kα radiation.

Time-Resolved Fluorescence Measurements

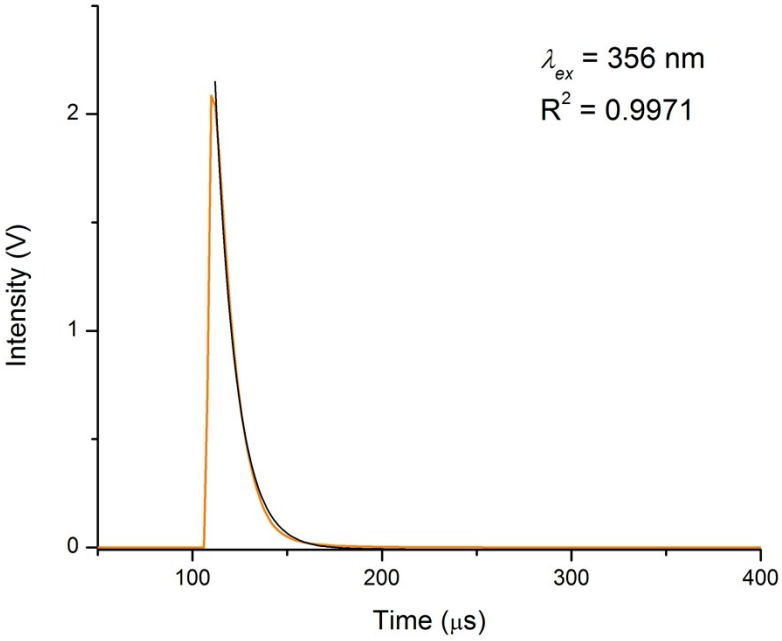

Figure S 31. Lifetime decay curve of **Sm-1** acquired at a lamp frequency of 300 Hz. Overlaid black line denotes the fit of the exponential curve.

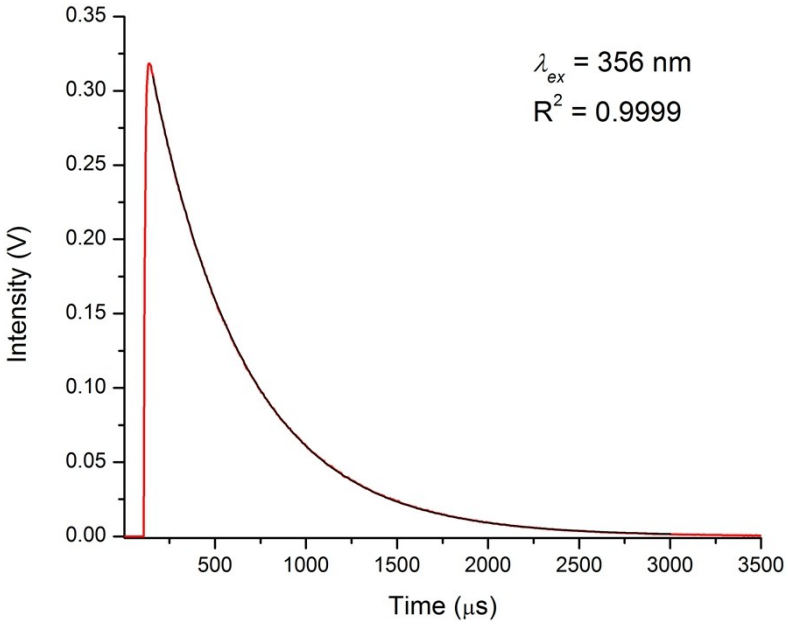

Figure S 32. Lifetime decay curve of **Eu-1** acquired at a lamp frequency of 200 Hz. Overlaid black line denotes the fit of the exponential curve.

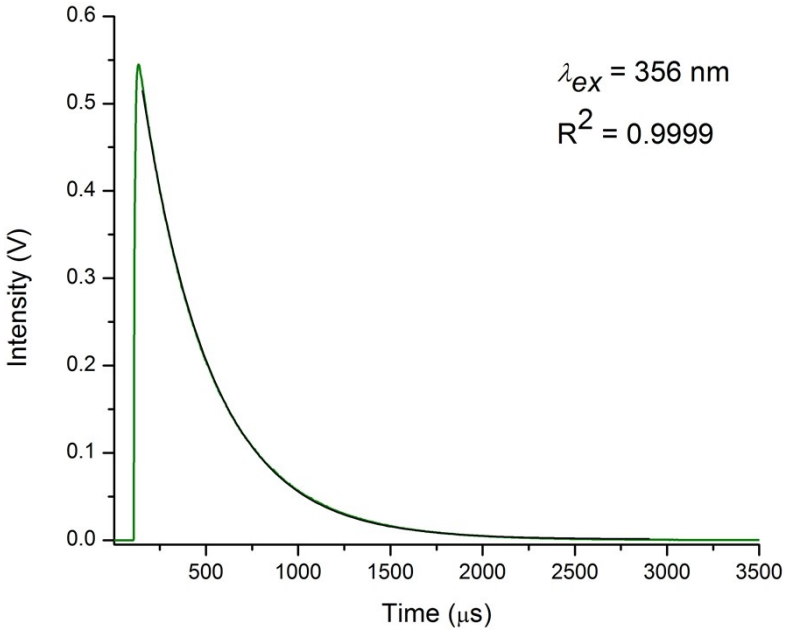

Figure S 33. Lifetime decay curve of **Tb-1** acquired at a lamp frequency of 200 Hz. Overlaid black line denotes the fit of the exponential curve.

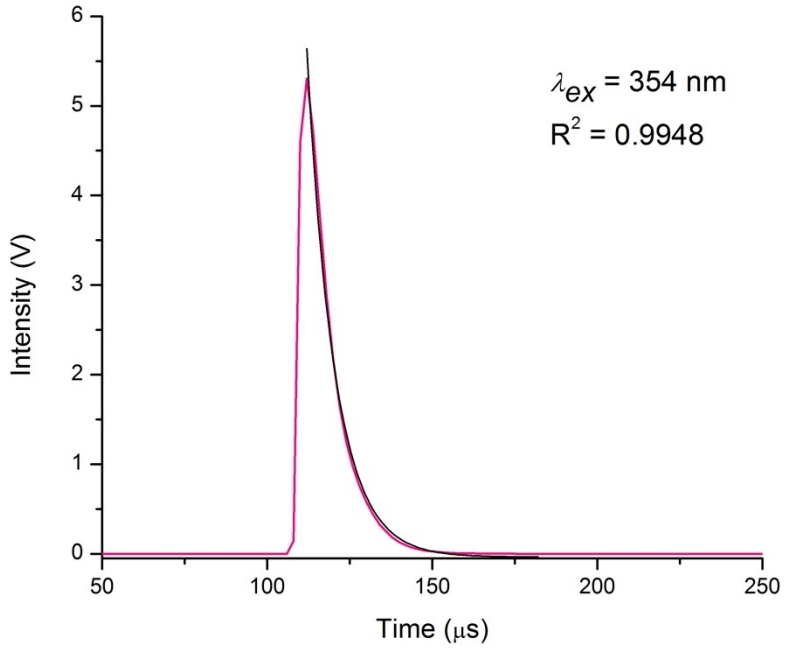

Figure S 34. Lifetime decay curve of **Dy-1** acquired at a lamp frequency of 300 Hz. Overlaid black line denotes the fit of the exponential curve.

Thermogravimetric Analysis

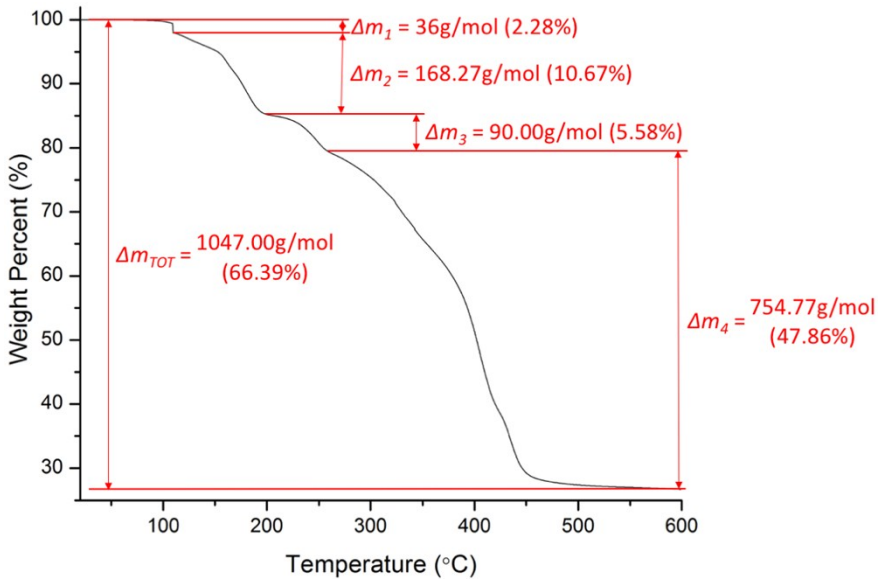

Figure S 35. TGA curve obtained for **Eu-1** under dinitrogen flow at a heating rate of 5 °C min^{-1}.

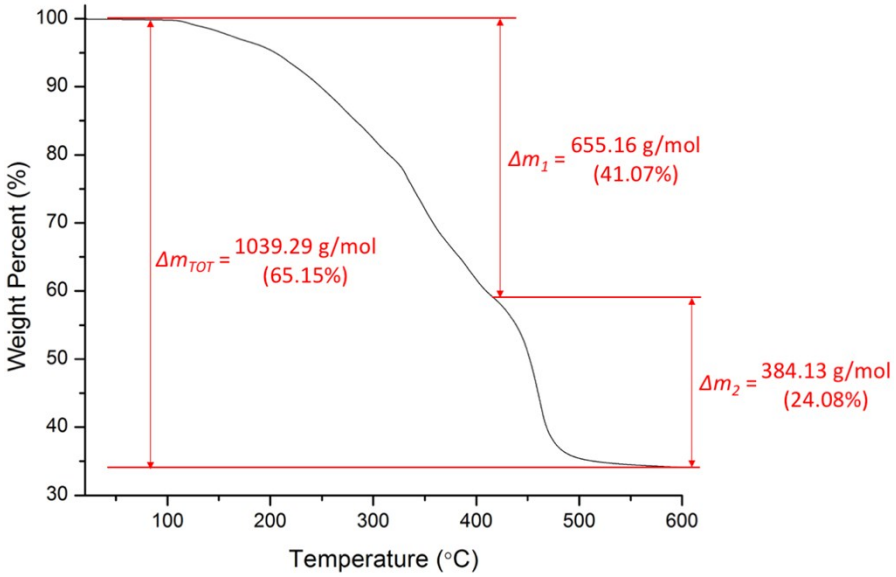

Figure S 36. TGA curve obtained for **Ho-2** under dinitrogen flow at a heating rate of 5 °C min^{-1}.

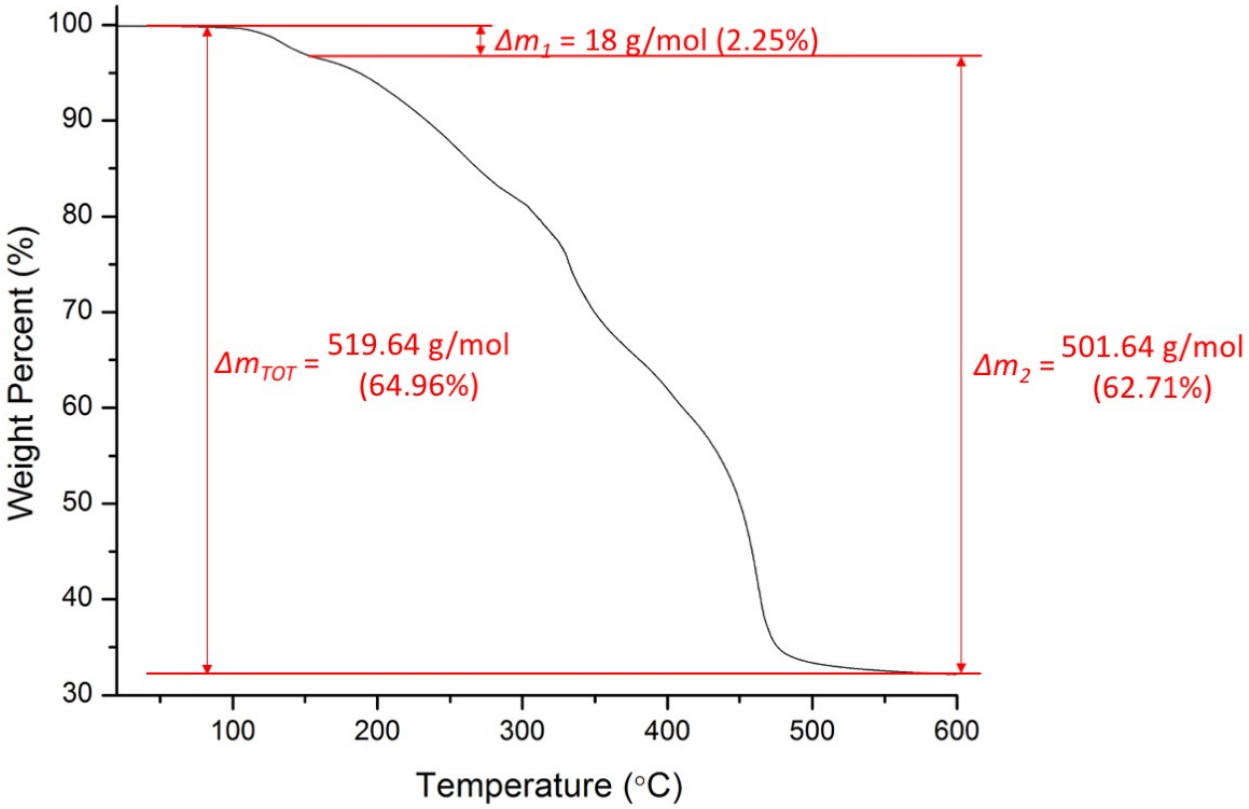

Figure S 37. TGA curve obtained for **Er-3** under dinitrogen flow at a heating rate of 5 °C min^{-1}.

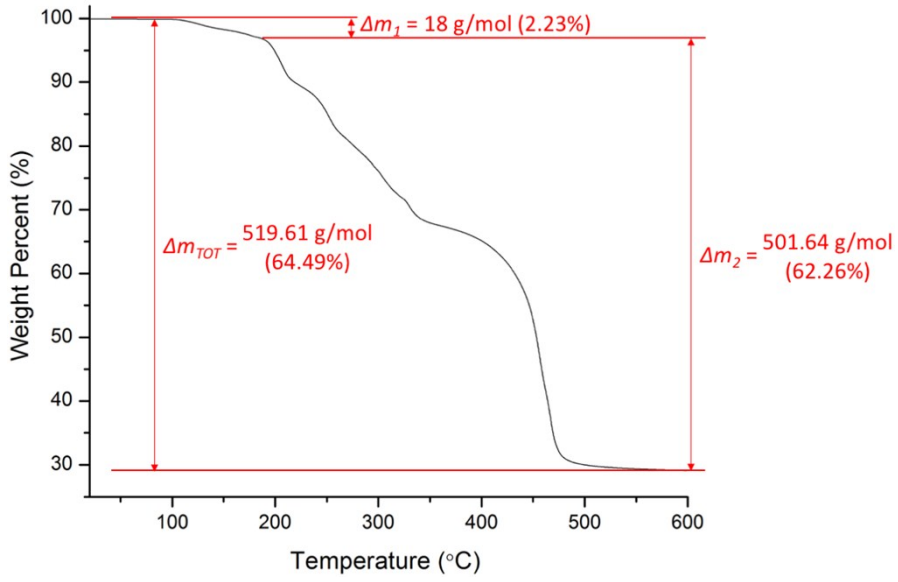

Figure S 38. TGA curve obtained for **Yb-4** under dinitrogen flow at a heating rate of 5 °C min^{-1}.

Infrared Spectra

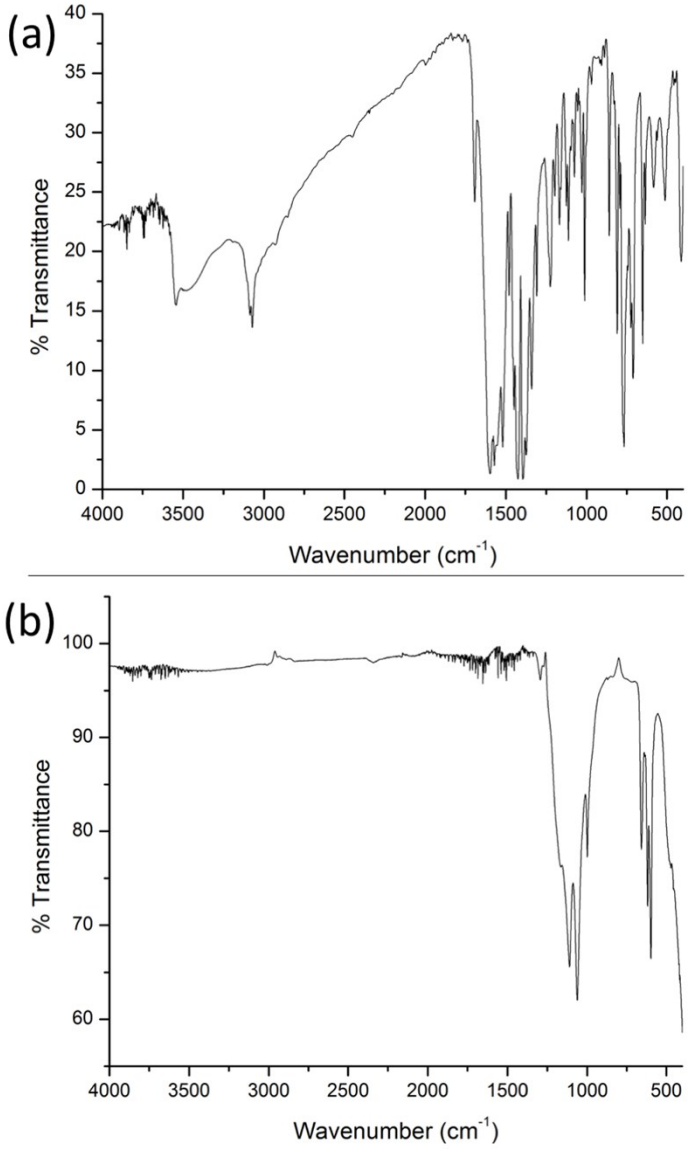

Figure S 39. FTIR spectra of (a) **Eu-1** and (b) product of thermal decomposition after thermogravimetric analysis. The peaks centered at 1063(bs), 666(s), and 600(s) cm^{-1} in (b) correspond to the sulfate ion asymmetric stretch, symmetric stretch, and asymmetric bend, respectively.

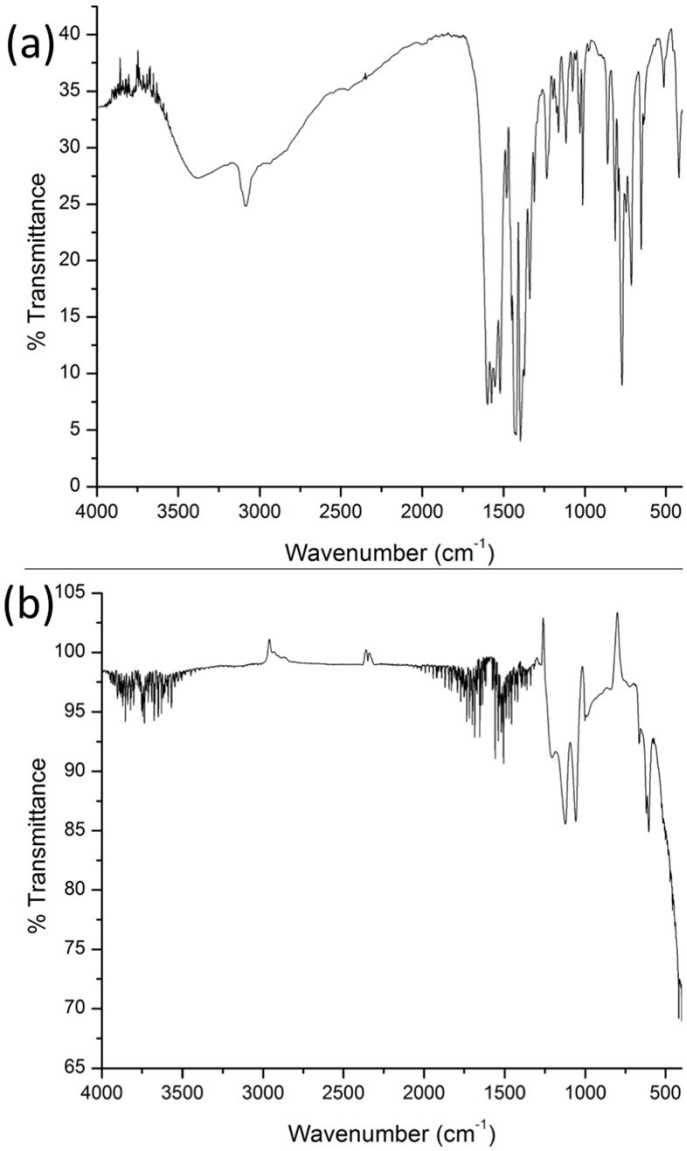

Figure S 40. FTIR spectra of (a) **Ho-2** and (b) product of thermal decomposition after thermogravimetric analysis. The peaks centered at 1125(bs), 665(w), and 605(s) cm^{-1} in (b) correspond to the sulfate ion asymmetric stretch, symmetric stretch, and asymmetric bend, respectively.

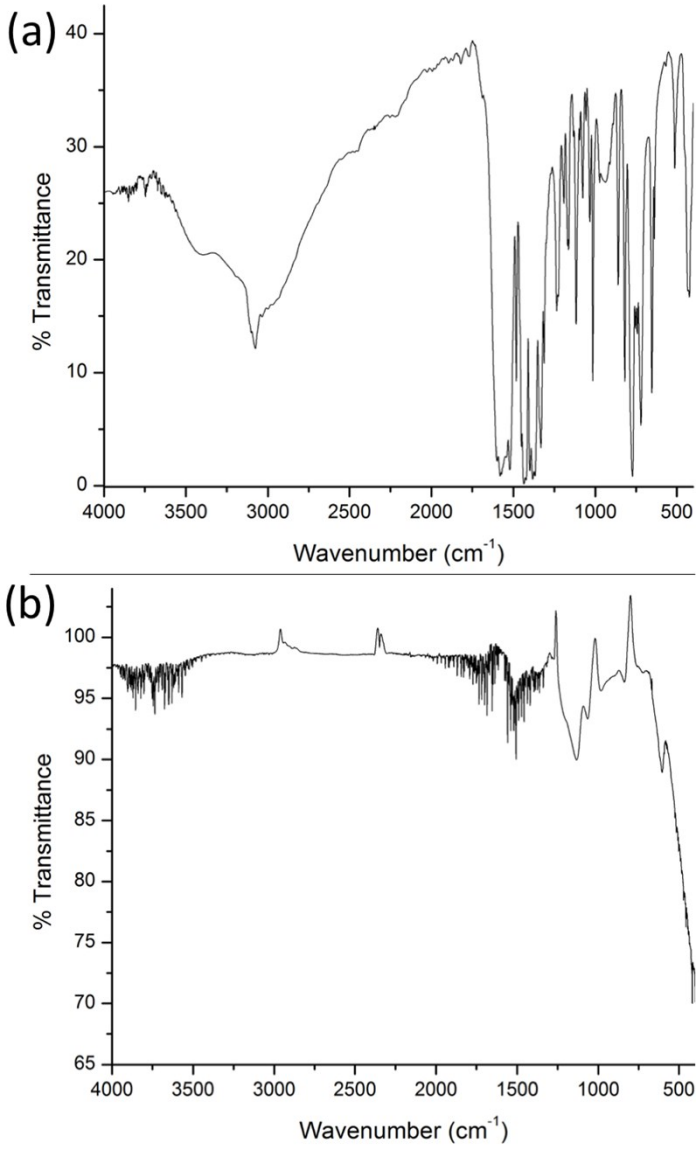

Figure S 41. FTIR spectra of (a) **Er-3** and (b) product of thermal decomposition after thermogravimetric analysis. Peaks centered at 1132(bs) and 604(s) cm^{-1} in (b) correspond to the sulfate ion asymmetric stretch and asymmetric bend, respectively.

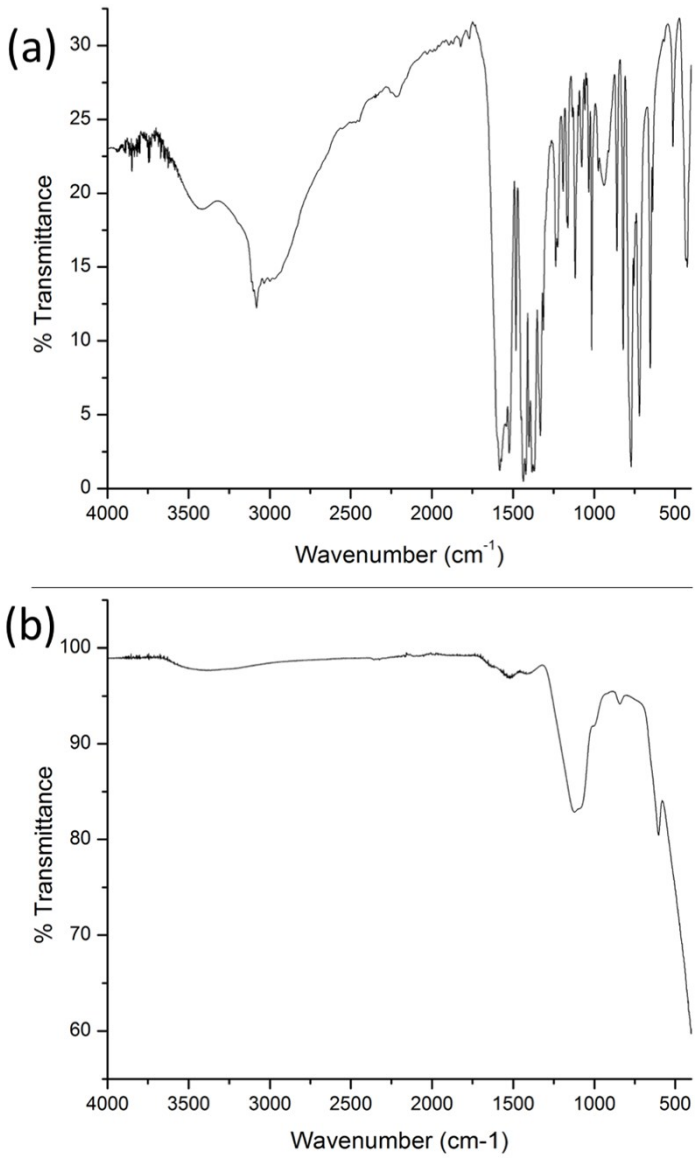

Figure S 42. FTIR spectra of (a) **Yb-4** and (b) product of thermal decomposition after thermogravimetric analysis. Peaks centered at 1126(bs) and 605(s) cm^{-1} in (b) correspond to the sulfate ion asymmetric stretch and asymmetric bend, respectively.